Front. Mater. Sci.
https://doi.org/10.1007/s11706-021-0566-4

LETTER

Large-scale synthesis of metal nanosheets as highly active catalysts: Combining accumulative roll-bonding and etching process

Yuxin OUYANG[1*], Juan LIU[2*], Yue XIN[1], Wenkun ZHU[3], Hailiang YU (✉)[2], and Liangbing WANG (✉)[1]

1 State Key Laboratory for Powder Metallurgy, Key Laboratory of Electronic Packing and Advanced Functional Materials of Hunan Province, School of Materials Science and Engineering, Central South University, Changsha 410083, China

2 State Key Laboratory of High Performance Complex Manufacturing, College of Mechanical and Electrical Engineering, Light Alloys Research Institute, Central South University, Changsha 410083, China

3 State Key Laboratory of Environment-friendly Energy Materials, National Co-innovation Center for Nuclear Waste Disposal and Environmental Safety, Nuclear Waste and Environmental Safety Key Laboratory of Defense, School of National Defence Science & Technology, Southwest University of Science and Technology, Mianyang 621010, China

E-mails: wanglb@csu.edu.cn (L.W.), yuhailiang@csu.edu.cn (H.Y.)

* Y.O. and J.L. contributed equally to this work.

Supplementary information

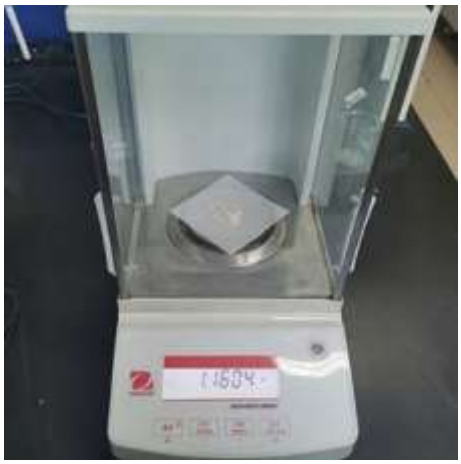

Fig. S1 Large-scale production of AgZn-E.

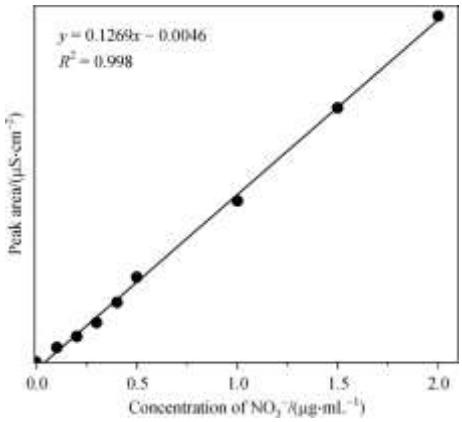

Fig. S2 The peak area of a series of NO_3^- solutions with distinct concentrations.

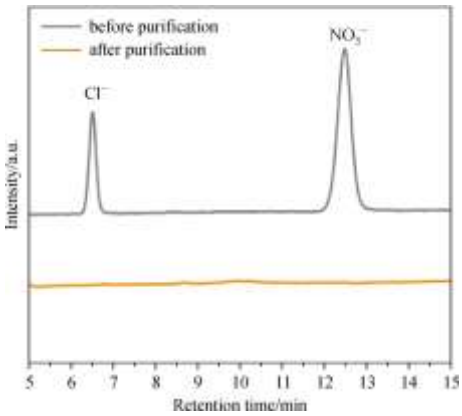

Fig. S3 Ion chromatograph spectra of catalysts before and after purification.

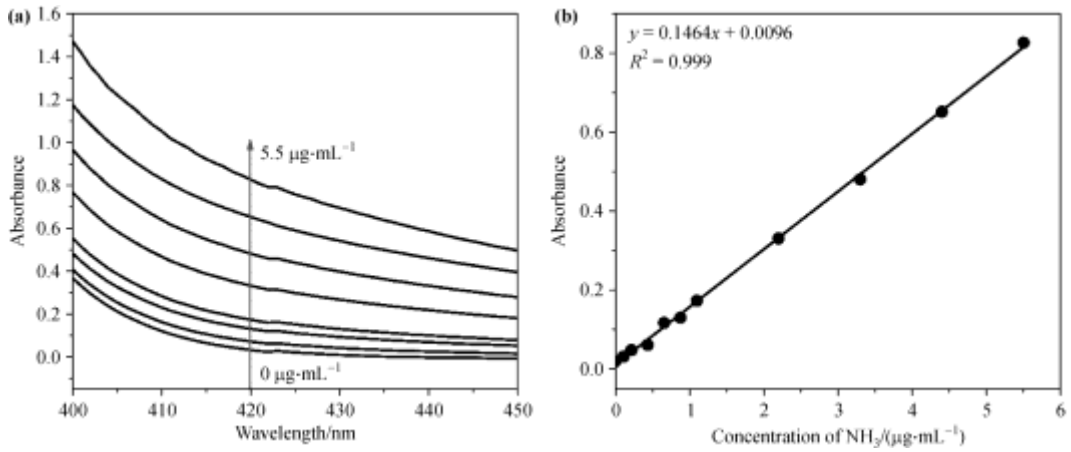

Fig. S4 (a) Extinction spectra and **(b)** the extinction at 420 nm of a series of NH_3 detected with distinct concentrations in Nessler's reagent method.

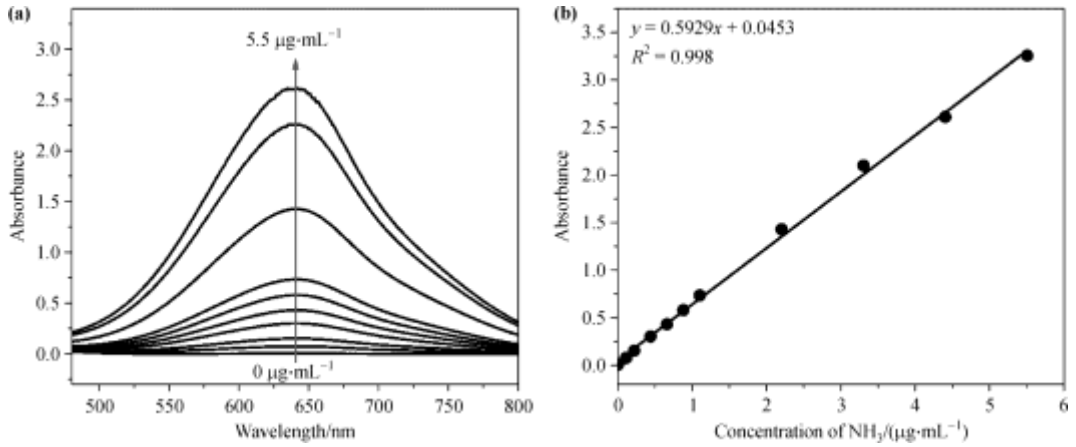

Fig. S5 (a) Extinction spectra and **(b)** the extinction at 639 nm of a series of NH_3 with distinct concentrations in indophenol blue method.

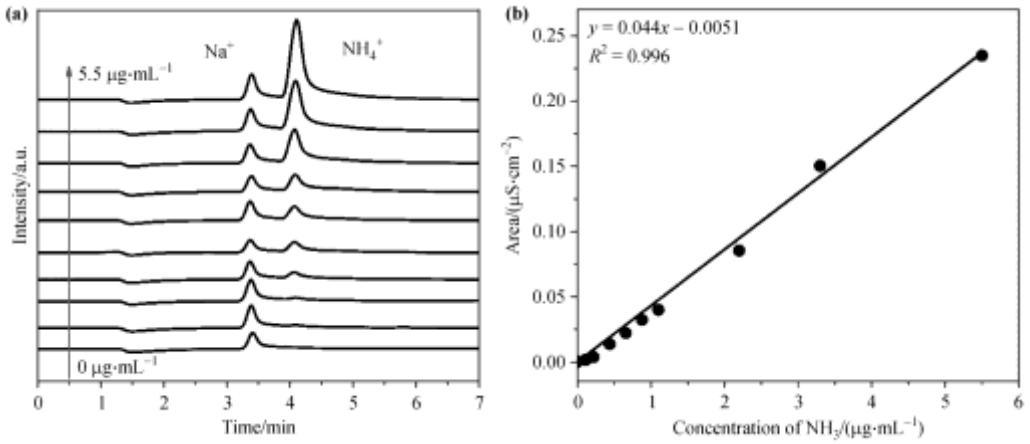

Fig. S6 (a) Ion chromatograph spectra and **(b)** peak areas of a series of NH_4^+ solutions with distinct concentrations.

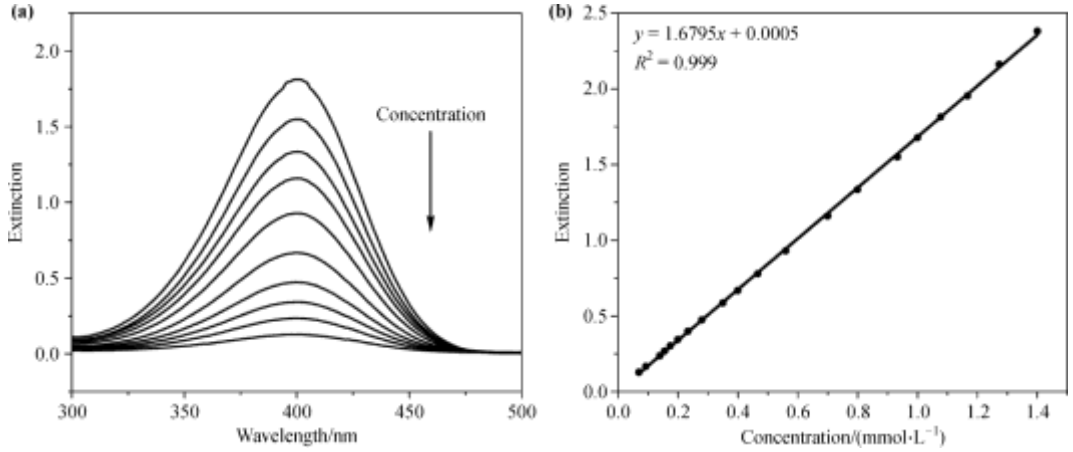

Fig. S7 (a) Extinction spectra and **(b)** the extinction at 400 nm of a series of p-nitrophenol solutions with distinct concentrations.

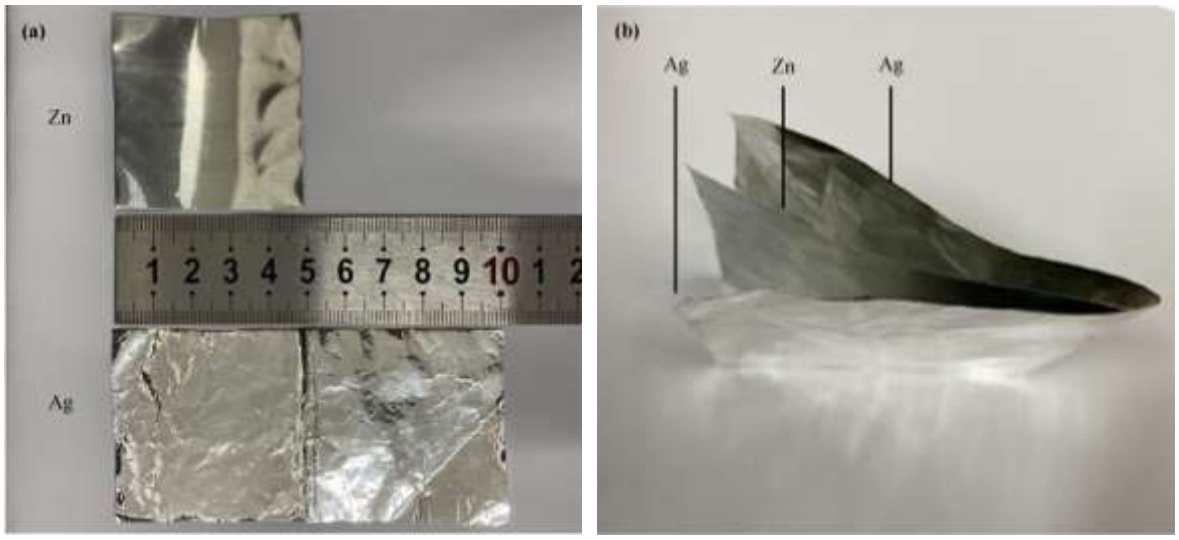

Fig. S8 (a) The original metallic zinc (50 mm × 50 mm × 0.07 mm) and metallic silver (100 mm × 50 mm × 0.015 mm). **(b)** The initial sandwich structure before accumulative roll-bonding.

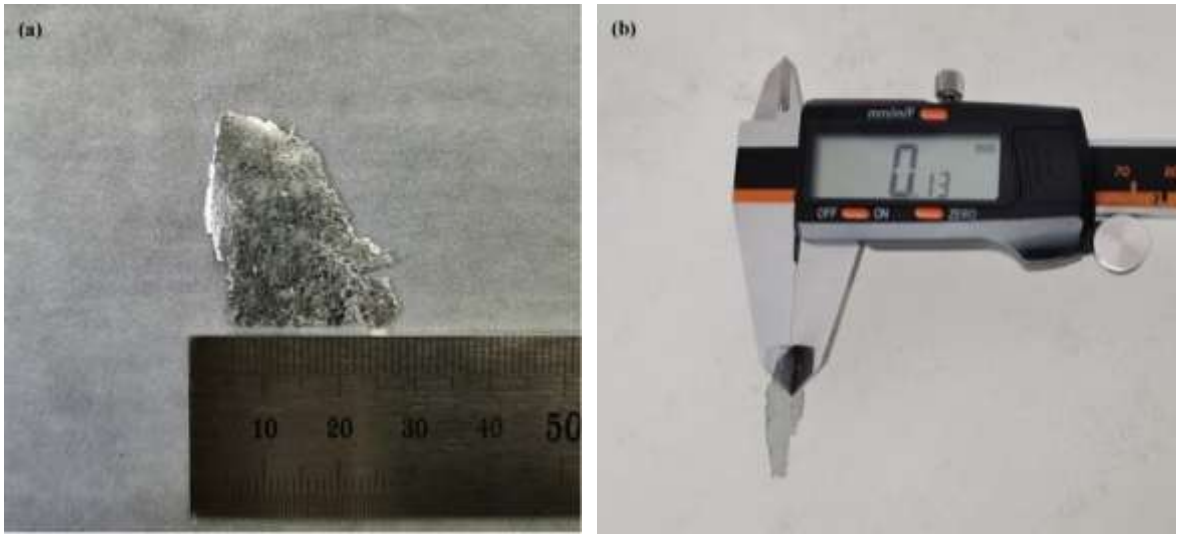

Fig. S9 (a) The obtained AgZn-R after 14 cycles of accumulative roll-bonding. **(b)** The thickness of obtained AgZn-R.

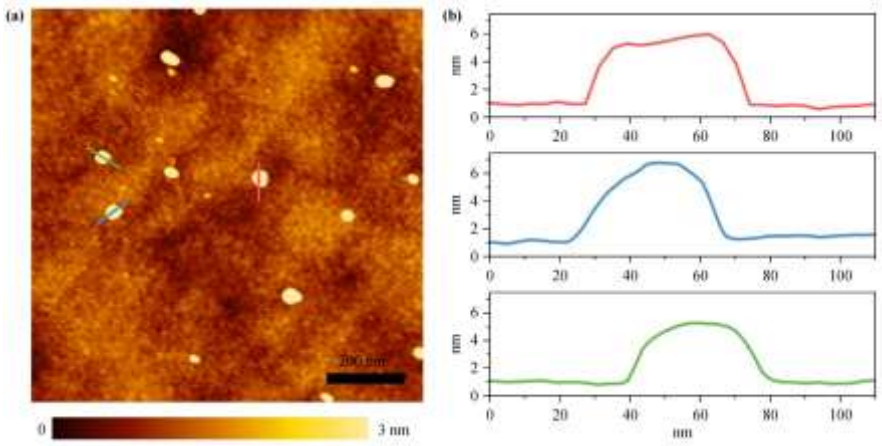

Fig. S10 (a) AFM image of AgZn-E. **(b)** Topographic height acquired in the location of left lines.

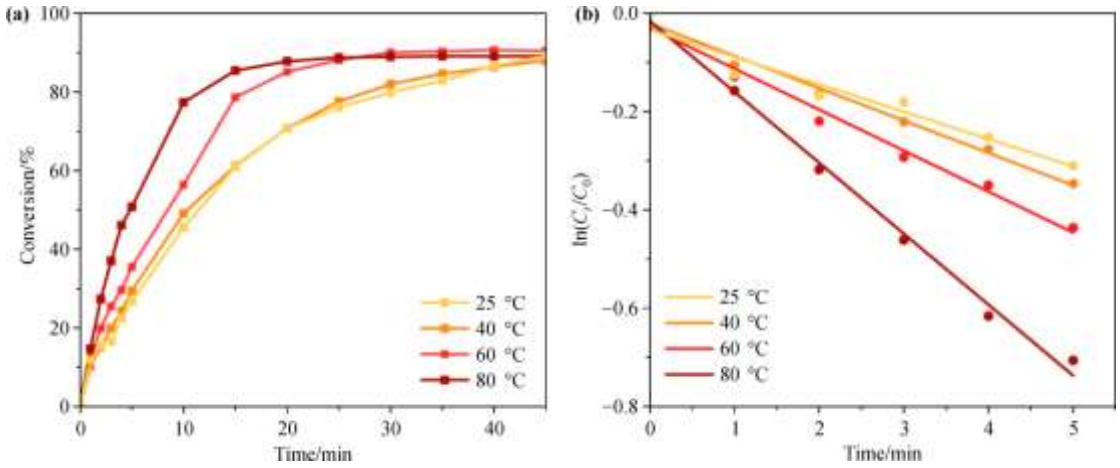

Fig. S11 (a) Conversion of p-nitrophenol and **(b)** plots of $\ln(C_t/C_0)$ *vs.* time over AgZn-E at different temperatures.

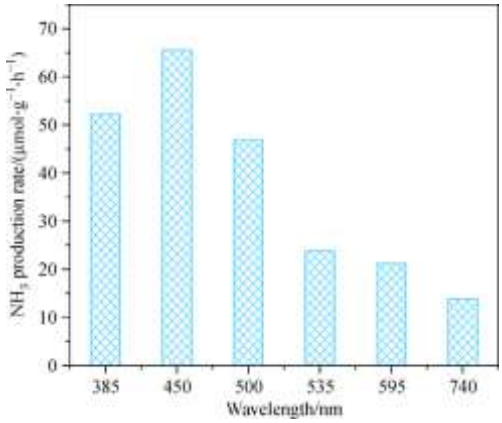

Fig. S12 NH_3 production rates for the N_2 fixation catalyzed by AgZn-E under monochromatic light with the wavelengths of 385, 450, 500, 535, 595 and 740 nm.

Table S1 Catalytic performance for the fixation of N_2 over AgZn-E detected by different methods

Method	NH_3 production rate/($\mu mol \cdot g_{cat.}^{-1} \cdot h^{-1}$)
Nessler's reagent	126.3
Indophenol blue	122.3
Ion chromatograph	123.6

Table S2 Reported catalytic performance for the fixation of N_2 by other photocatalysts

Catalyst	NH_3 production rate /($\mu mol \cdot g_{cat.}^{-1} \cdot h^{-1}$)	NH_3 production rate /($\mu mol \cdot L^{-1} \cdot h^{-1}$)	NH_3 production rate /($\mu mol \cdot g_{cat.}^{-1} \cdot L^{-1}$)
AgZn-E	126.3	63.2	3157.5
H-Bi_5O_{71}	162.5		
r-GO@$H_5[PMo_{10}V_2O_{40}]$		130.3	
ZIF-67@$K_{11}[PMo_4V_8O_{40}]$		149.0	
ZnS/GO			910.6
0.4BWO/g-C_3N_4		535.9	
Ru/TiO_2	3.3		